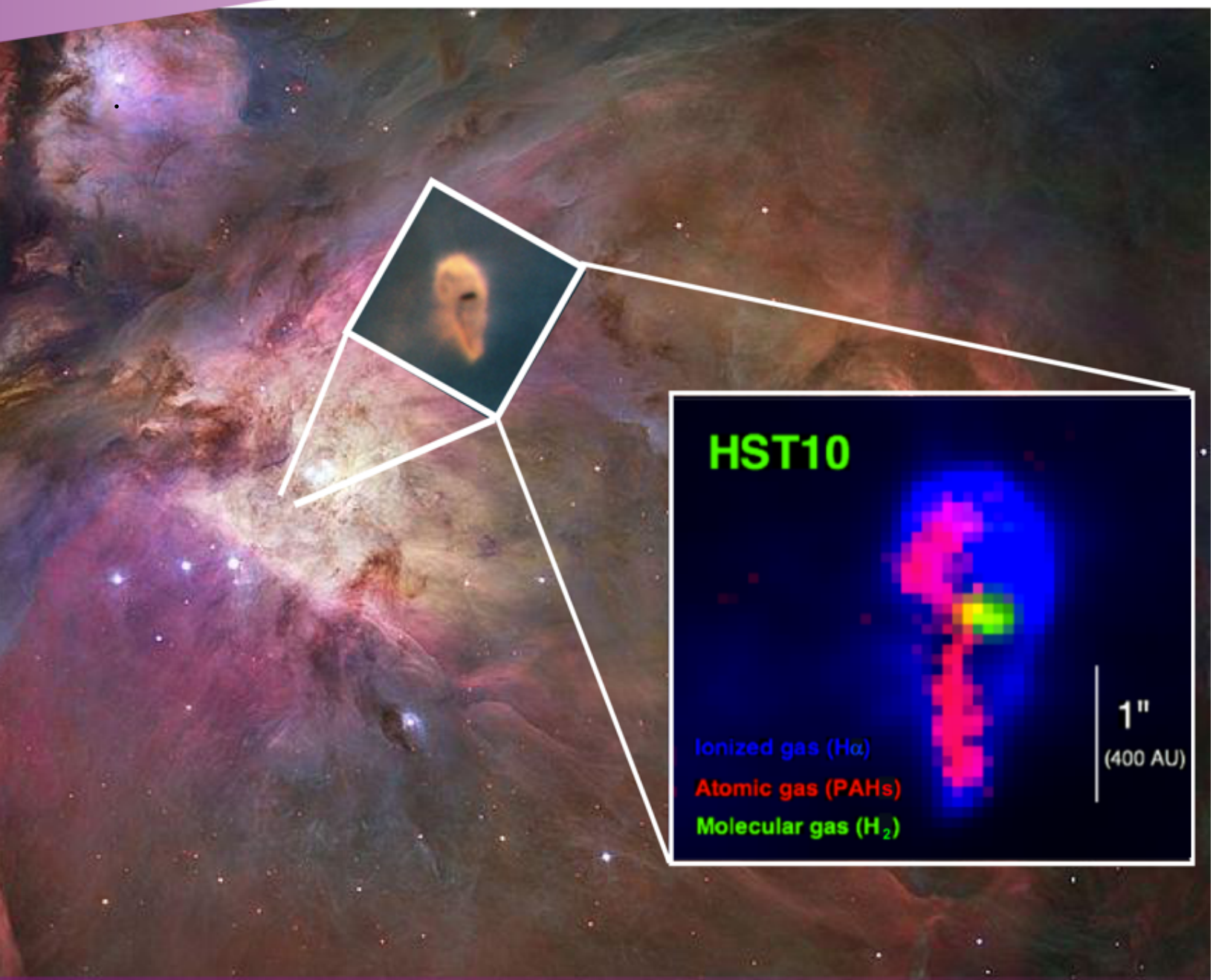


AstropAH

A Newsletter on Astronomical PAHs

Issue 39 | June 2017



HST10

Ionized gas (H α)

Atomic gas (PAHs)

Molecular gas (H $_2$)

1"
(400 AU)

Editorial

Dear Colleagues,

We open our June issue with the amazing images of the beautiful Orion Nebula and one of its proplyds.

In the *In Focus*, Andy Mattioda shows us the results of a recently concluded spectroscopic study of Polycyclic Aromatic Nitrogen Heterocycles (PANHs).

This issue showcases abstracts of observational, experimental and theoretical works about the structure, stability and spectroscopic properties of different PAHs and PAH-related molecules, including a computational study about DNA in non-terran environments.

AstroPAH can help you promote your science. Visit our webpage or contact us for more information. You can send us your contributions anytime. For publication in July, see the deadlines below.

We thank you all for your contributions so far!

The Editorial Team

**Next issue: 18 July 2017.
Submission deadline: 7 July 2017.**

AstroPAH Newsletter

Editorial Board:

Editor-in-Chief

Prof. Alexander Tielens

Leiden Observatory
(The Netherlands)

Executive Editor

Dr. Isabel Aleman

IAG-USP, University of São Paulo
(Brazil)

Editors

Dr. Alessandra Candian

Leiden Observatory
(The Netherlands)

Dr. Elisabetta Micelotta

Department of Physics
University of Helsinki (Finland)

Dr. Annemieke Petrignani

University of Amsterdam
(The Netherlands)

Dr. Ella Sciamma-O'Brien

NASA Ames Research Center (USA)

Dr. Amanda Steber

Max Planck Institute for the Structure
and Dynamics of Matter (Germany)

Contact us:

astropah@strw.leidenuniv.nl

<http://astropah-news.strw.leidenuniv.nl>

[Click here to Subscribe to AstroPAH](#)

[Click here to Contribute to AstroPAH](#)

Contents

PAH Picture of the Month	1
Editorial	2
In Focus	4
Recent Papers	12

PAH Picture of the Month

Composite color image of the externally illuminated protoplanetary disk (or proplyd) HST10. In blue (and in yellow in the central inset) $H\alpha$ emission tracing the ionized gas at the ionization front, in green H_2 , tracing the molecular gas at the surface of the nearly edge-on protoplanetary disk, and in red the PAH emission at $11\ \mu\text{m}$. See [Vicente et al., ApJL, 2013, 765:L38](#) for more informations. Proplyds like HST10 are very common in star forming region, like the Orion Nebula (Background image).

Credits: Background. NASA/ ESA, M. Roberto (STSCI/ESA) and the Hubble Space Telescope Orion Treasury Project Team. Central inset. NASA, C.R. O'Dell and S.K. Wong (Rice University). Image composition by Alessandra Candian.



Infrared spectroscopy of matrix-isolated neutral polycyclic aromatic nitrogen heterocycles: The acridine series

presented by **Andy Mattioda**

Motivated in large part by our multi-decade investigation into the molecular spectroscopy of PAHs (Polycyclic Aromatic Hydrocarbons), we have just concluded an in-depth spectroscopic study of a subgroup of PAHs containing nitrogen. Why nitrogen? Well, nitrogen is the 4th most abundant chemically reactive element in space. The nitrogen atom is able to replace a CH group and participate in the aromatic bonding of the molecule, helping to maintain the PAHs robust structure. Furthermore, evidence has been mounting that these Polycyclic Aromatic Nitrogen Heterocycles (PANHs) could be present in space (Peeters et al. 2003, Mattioda et al. 2003, Hudgins & Allamandola 2004, Hudgins et al. 2005). PANHs have been detected in meteorites (Stoks & Schwartz, 1982, Pizzarello 2001) and they are believed to be a component of Titans haze (Ricca et al. 2001). If PANHs are part of the PAH inventory of the ISM, it would have very interesting astrobiological implications due to PANH molecules being involved in many biological processes. Thus, the presence of PANHs in the ISM would imply their availability to habitable bodies throughout the universe (Kuan et al. 2003).

Our past work with PANH Mid-IR spectroscopy identified the increase in the CH out-of-plane (CHoop) band intensities (1100 - 1600 cm⁻¹ or 9.09 - 6.25 μm) (Mattioda et al. 2003) compared to the parent PAH. This two fold increase in intensity is a result of the higher electronegativity of the nitrogen atom disrupting the homogenous aromatic electron cloud found in a typical, neutral PAH, similar to what happens upon ionization of a PAH. This earlier work also identified an intense band occurring around 1400 cm⁻¹ (7.14 μm) due to the nitrogen substitution. Upon ionization, the PANH molecules exhibited overall band intensities similar to the ionized parent PAH. The fact that nitrogen substitution somewhat mimics the effect of ionization in PAHs impedes the analysis of ion bands as they tend to occur very close to the neutral band positions in the PANHs. Additionally, we reported the identification of the first PANH anion for the phenazine molecule (Mattioda et al. 2005), which contains a dual nitrogen substitution.

Additional PANH mid-IR studies include those of Gao et al. 2016 and Hudgins et al. 2005. Both studies involve the use of PANHs to explain variations in the 6.2 μm PAH features. The

theoretical study by Hudgins et al. (Hudgins et al. 2005) found that incorporation of nitrogen atom internally (endo-skeletal) in a large PAH structure can explain the observed 6.2 μm shift. (Gao et al. 2016) investigated the influence of metal ion binding with the PANH noting that the strong CNC stretch of undergoes a $\sim 20\text{ cm}^{-1}$ redshift away from the 6.2 μm position when complexed with a copper ion.

Our current investigation (Mattioda, et al., 2017) follows the growth of the PAH anthracene through the addition of benzene rings to create benz[a]anthracene and various forms of dibenzanthracene as well as the corresponding nitrogen substitution. The creation of bay regions in the PAH structure via the benzene ring additions is discussed as is the incorporation of the nitrogen atom into the structure. The structures studied are provided in Fig. 1. For ease of review the IR spectrum is divided into the characteristic PAH regions of skeletal modes ($<700\text{ cm}^{-1}$); CHoop region ($700\text{-}1000\text{ cm}^{-1}$); C-C, C-H in-plane region ($1000\text{-}1650\text{ cm}^{-1}$) and the C-H stretching region ($3000\text{-}3110\text{ cm}^{-1}$). The following paragraphs summarize the important findings of this article.

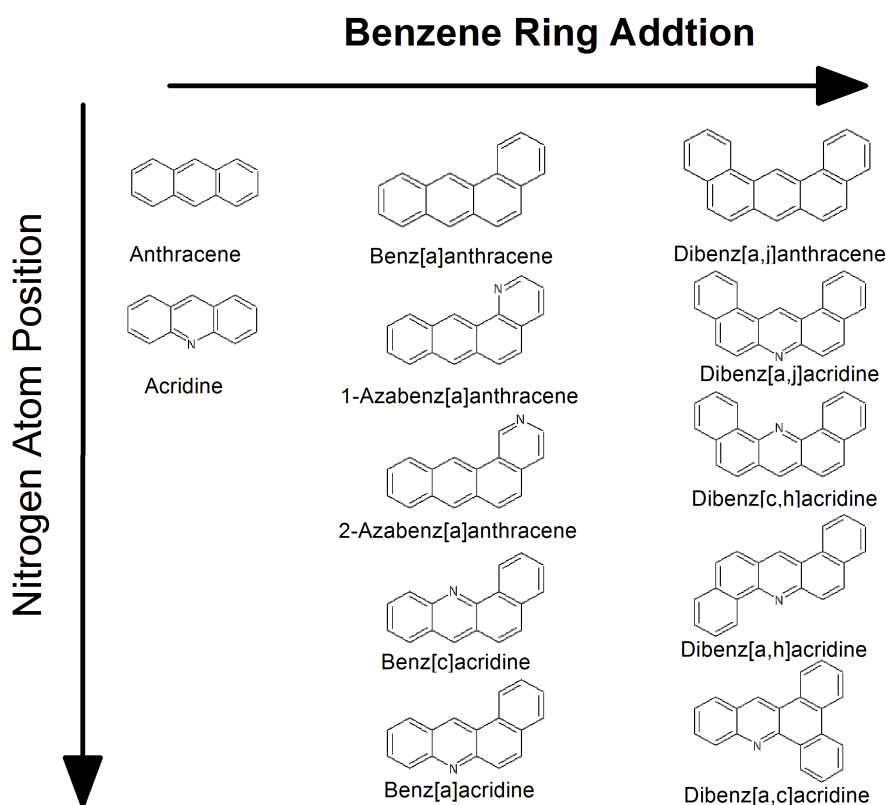


Figure 1: PAH and PANH structures in this investigation.

Far infrared (IR) modes

A minor, but interesting outcome of this investigation concerns the Far IR modes occurring between 450 cm^{-1} and 700 cm^{-1} . The vibrational modes in this region are weak, with A values generally less than $\sim 10\text{ KM/Mole}$ in intensity. Anthracene exhibits the simplest spectrum in this

region, with only two visible modes. However, the addition of a benzene ring as well as the incorporation of nitrogen atom increases the number of modes in this region to 5 ± 1 (See Fig. 2). While the addition of a single benzene ring, creating benz[a]anthracene, increases the number of visible modes. The addition of a second benzene ring, creating a dibenz[x,y]anthracene does not result in the appearance of additional bands in this region but does result in band position shifts.

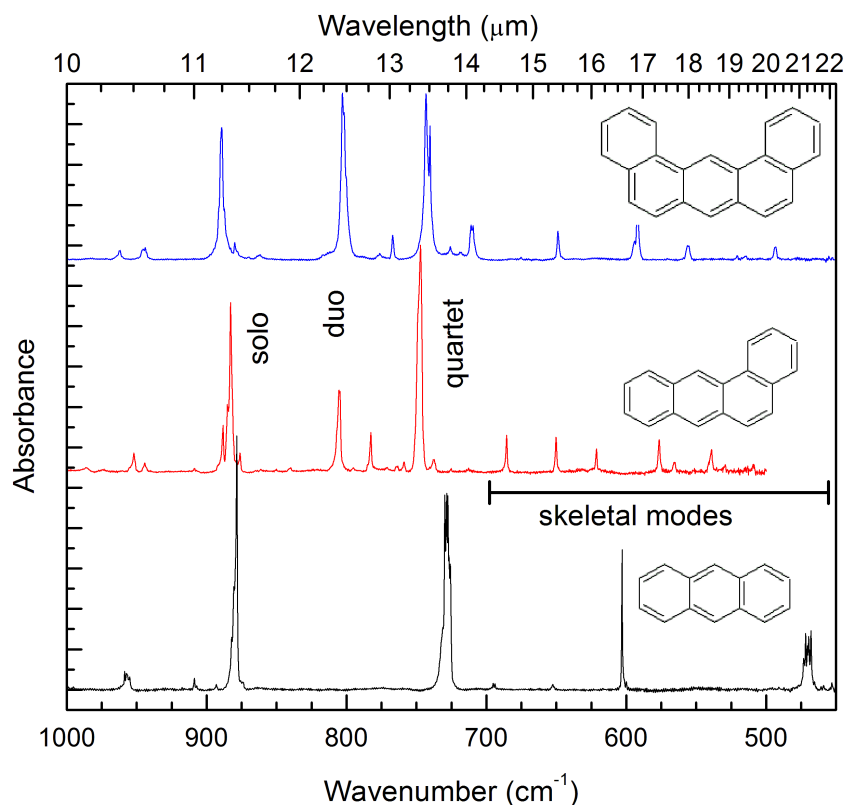


Figure 2: Changes in the 10-20 μm region upon addition of benzene rings, creating bay regions in a PAH. Note the increase in the number of skeletal modes, the creation of the duo modes and the shifting of the solo and quartet modes.

CH out-of-plane (CHoop) modes

The 10-15 μm region ($667\text{-}1000\text{ cm}^{-1}$) is known as the C-H out-of-plane (CHoop) region in PAH spectroscopy, identifying the singly adjacent (solo), doubly adjacent (duo), triply adjacent (trio) and quadruple adjacent (quartet) C-H groups (Hudgins & Allamandola, 1999). According to Hudgins and Allamandola (1999), one can identify the C-H groups based on the frequency (wavelength) of the vibrational band. The solo hydrogen C-H groups typically fall in the $900\text{ to }860\text{ cm}^{-1}$ ($11.1\text{-}11.6\text{ }\mu\text{m}$) range, the duo hydrogen groups into the $810\text{-}750\text{ cm}^{-1}$ ($12.4\text{-}13.3\text{ }\mu\text{m}$) range, the trio hydrogen groups into the $770\text{-}735\text{ cm}^{-1}$ ($13\text{-}13.6\text{ }\mu\text{m}$) and the quartets into two regions, one at $770\text{-}730\text{ cm}^{-1}$ ($13.13\text{-}13.7\text{ }\mu\text{m}$) and $710\text{-}690\text{ cm}^{-1}$ ($14.1\text{-}14.5\text{ }\mu\text{m}$).

While our recent work, including this current PANH study, have noted considerable coupling between the various C-H groups (e.g. solo, duo, trio, quartet) in the CHoop region, the solo,

duo, trio and quartet nomenclature is still useful when discussing the infrared spectra. The IR spectra of the non-nitrogenated, parent, PAHs are presented in Fig. 2. Anthracene, which contains only quartet and solo modes, exhibits bands at 727.6 and 878.3 cm^{-1} due to the quartet and solo CHoop modes. Addition of a benzene ring (benz[a]anthracene) creates a duo CHoop group exhibiting a band at 805.4 cm^{-1} , while the addition of a second benzene ring, creating dibenz[a,j]anthracene, adds a second duo CHoop group, increasing the intensity of this band. It is interesting to note that the addition of benzene rings causes a blue shift to the solo CHoop vibrational modes. Likewise, it is important to note that the dibenz[a,j]anthracene PAH molecule exhibits one of the rare disagreements between theory and experiment. Theory predicts a strong solo mode at 847.9 cm^{-1} whereas the strongest experimental mode is seen at 889.3 cm^{-1} (see Table 4 in Mattioda et al. 2017). Changing basis sets for the theoretical calculation did not resolve this issue, but did shift the theoretical band to higher frequencies. The experimental spectrum does contain bands near the theoretical values, which seems to suggest this may be an example of either theory obtaining a poor intensity or the matrix-isolated experimental band intensity being much smaller than observed in the gas phase. Addition of a benzene ring also shifts the quartet mode to the blue for the first addition. The addition of a second benzene ring, (dibenz[a,j]anthracene) splits the solo vibrational mode between the bay region solo C-H group and the external solo C-H group, with the external group being responsible for the intense mode at 889.3 cm^{-1} . While the external solo C-H group couples to the adjacent duo C-H groups, the bay solo C-H group couples to the adjacent quartet C-H groups.

The separation and coupling of the solo C-H groups into bay and external ones, provides a spectroscopic tool for interpreting the nitrogen substituted benz[a]anthracene and dibenz[a,j]-anthracene infrared spectra, helping to simplify the explanation for a complicated situation. Figure 3 shows the IR spectra for benz[a]anthracene and related PANH molecules. As can be seen in the figure, these PAH species contain an IR band around 750 cm^{-1} (13.3 μm) corresponding to the quartet C-H groups. A nitrogen substitution on the attached benzene ring (e.g. 1- and 2-azabenz[a]anthracene) does not produce a shift in the quartet mode but does decrease the intensity of this band. This decrease in intensity is most likely due to the loss of one set of the quartet C-H groups by the nitrogen substitution. In contrast, nitrogen substitution in the acridine position results in a blue shift of the quartet mode, regardless of if the nitrogen atom is internal or external to the bay region. The duo mode around 805.4 cm^{-1} (12.4 μm) provides additional information, as well, regarding nitrogen substitution in benz[a]anthracene. For benz[c]acridine, 2-azabenz[a]anthracene and 1-azabenz[a]anthracene this band shifts slightly to the red ($\sim 3 \text{ cm}^{-1}$), while a significant blue shift is observed ($\sim 30 \text{ cm}^{-1}$) for the benz[a]acridine. This drastic difference arises from the strong out-of-phase coupling between the duo C-H groups and the external solo C-H group.

Dibenz[a,j]anthracene, dibenz[a,j]acridine and dibenz[c,h]acridine are structurally identical with the exception of the presence and position of the nitrogen atom (see Fig. 1). The IR spectra for these molecules are shown in Fig. 4. The quartet band shifts slightly to the blue regardless of whether the nitrogen atom replaces the bay or external solo C-H group. However, this is not the case with the duo CHoop mode. For dibenz[c,h]acridine, where the nitrogen atom replaces the solo bay C-H group, there is very little, if any, change in the band position from that observed for the parent PAH. This is not the case when the nitrogen atom replaces the

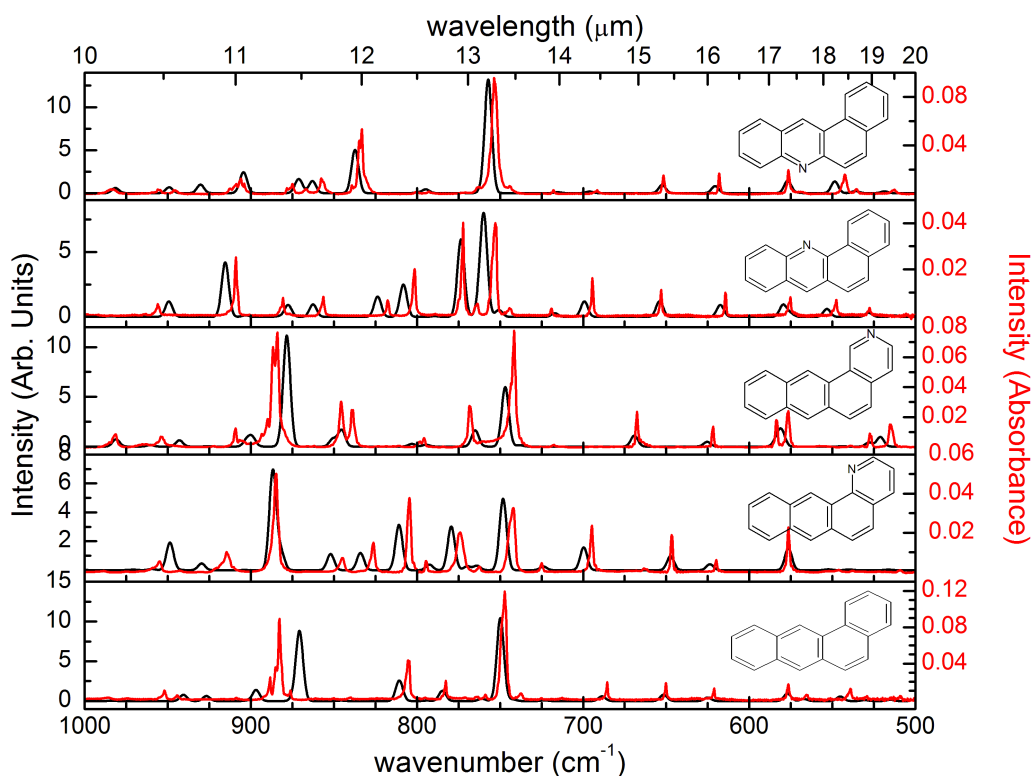


Figure 3: The 500-1000 cm^{-1} (CHoop and skeletal) region of the experimental (red) and theoretical (black) spectra for the benz[a]anthracene species. The experimental spectra have been normalized to 1×10^{16} molecules. Taken from Mattioda, et al. (2017).

external solo C-H group creating dibenz[a,j]acridine. Due to the coupling between the external solo C-H group and the adjacent duo C-H groups, replacement of the solo group with a nitrogen atom results in a dramatic $\sim 35 \text{ cm}^{-1}$ blue shift as well as a significant increase in the duo modes band intensity. The solo CHoop mode exhibits similar dramatic changes with nitrogen substitution. As previously mentioned, for dibenz[a,j]anthracene the solo CHoop mode is split between the external solo C-H group and the bay solo C-H group, with the higher frequency and intensity mode due to the external solo group. Thus, as was observed for the benz[a]anthracene series, when a nitrogen atom replaces the external solo C-H group this mode shifts $\sim 20 \text{ cm}^{-1}$ to the blue and is significantly reduced in intensity.

C-C, C-H in-plane modes

Perhaps one of the more intriguing aspects of the neutral PANH infrared spectrum was the discovery that the C-C, C-H in-plane region, $1100\text{-}1600 \text{ cm}^{-1}$ ($9.09\text{-}6.25 \text{ }\mu\text{m}$), exhibits a two-fold increase in intensity upon nitrogen incorporation into the carbon skeleton, while the intensity of the C-H stretching region, $3000\text{-}3120 \text{ cm}^{-1}$ ($3.33\text{-}3.20 \text{ }\mu\text{m}$), decreases slightly and the intensity of the CHoop region, $500\text{-}1100 \text{ cm}^{-1}$ ($20.0\text{-}9.09 \text{ }\mu\text{m}$) remains essentially unchanged, similar to what happens upon ionization of a PAH (Mattioda et al. 2003). The PANH acridine series is no different, following essentially the same trend (see Table 6 in Mattioda, et al. 2017). However, this current acridine study allowed us to further refine our observations. The majority of the

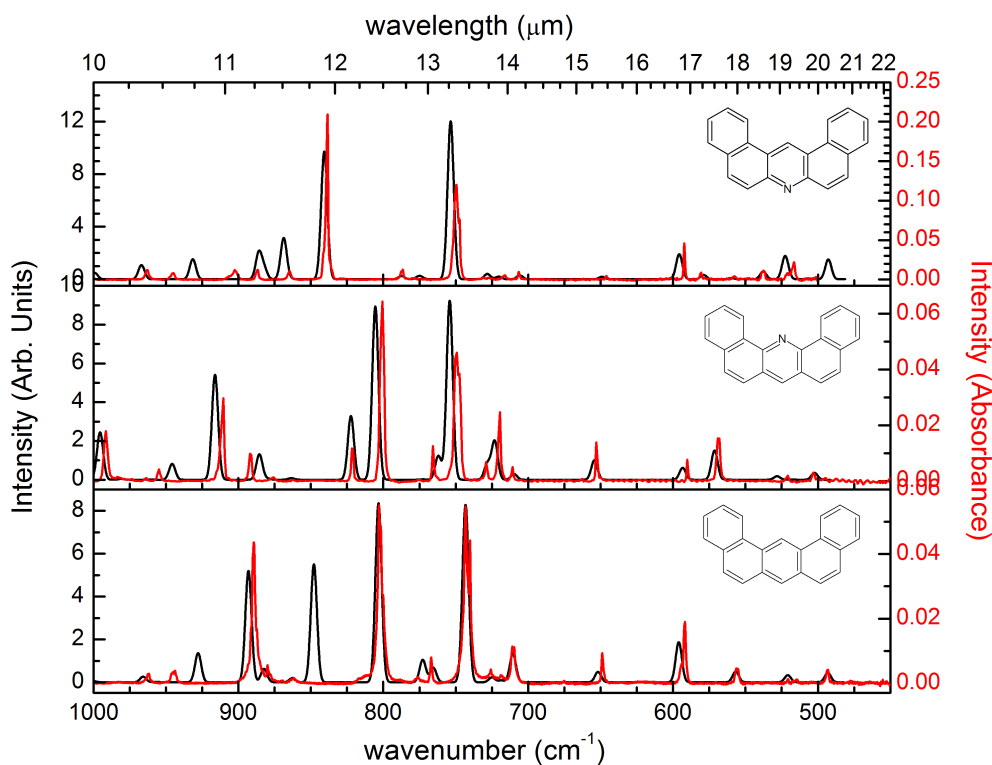


Figure 4: The 500-1000 cm^{-1} (CHoop and skeletal) region of the experimental (red) and theoretical (black) spectra for the dibenz[a,j]anthracene species. The experimental spectra have been normalized to 1×10^{16} molecules. Taken from Mattioda, et al. (2017).

C-C, C-H increase in band intensity falls in a very narrow range, 1375 to 1600 cm^{-1} (4.37-6.25 μm), with the intensity in this region ranging from 2 to 6 times that over the parent PAH when measured experimentally, and from 2 to 8 times in theoretical calculations.

Likewise, our earlier PANH work noted a very strong band around 1400 cm^{-1} (7.14 μm) due to a C-N-C rocking motion which results from a nitrogen atom para (opposite) an in-plane, solo, C-H group. The dibenz[a,j]acridine, dibenz[c,h]acridine, dibenz[a,h]acridine and dibenz[a,c]acridine PANHs all exhibited such a feature, while acridine, dibenz[a]acridine and dibenz[c]acridine did not. Upon further investigation, we noticed these three acridine PANHs did exhibit an intense band in the ~ 1480 -1515 cm^{-1} (6.76-6.60 μm) range. This vibrational band is a result of a C-N-C asymmetric stretch with a para hydrogen. Looking back at our 2003 PANH study, we noticed that 1-azachrysene, which did not exhibit the ~ 1400 cm^{-1} intense band, contained an intense mode around 1478 cm^{-1} (6.76 μm). In short, if a PANH molecule contains a hydrogen para to the nitrogen atom, it will exhibit an intense vibrational band around 1400 cm^{-1} (7.14 μm) and/or between ~ 1480 -1515 cm^{-1} (6.76-6.60 μm).

CH stretching modes

The aromatic C-H stretching region, running from 3,000 to 3,120 cm^{-1} (3.33 to 3.20 μm), is perhaps the most studied PAH IR region, astronomically speaking. Although the region is most commonly used only to identify the presence of aromatic species, due to the broadness of the

bands, recent theoretical and experimental studies have demonstrated much more structural information can be gleaned from this region (Mattioda, et al. 2014, Mackie, et al. 2016). This acridine study builds on this analysis. First, it is interesting to note that almost every PAH/PANH species studied in this investigation exhibited a band around 3020 cm^{-1} ($3.31\text{ }\mu\text{m}$). According to the Mackie et al. (2016) paper, this is a combination band resulting from C-C and C-H in-plane bends, at least in the benz[a]anthracene molecule. The remainder of the C-H stretching region is best summed up in Fig. 5. In this, and earlier studies, we note most aromatic C-H stretches due to solo C-H groups, fall in the 3040 to 3050 cm^{-1} (3.29 - $3.28\text{ }\mu\text{m}$), while those from the quartet C-H groups occur between 3070 - 3080 cm^{-1} (3.26 - $3.25\text{ }\mu\text{m}$). The region between 3050 and 3070 cm^{-1} (3.28 - $3.26\text{ }\mu\text{m}$) consists of combinations of duo, trio, and quartet bands. Finally, bands in the 3080 to 3110 cm^{-1} (3.25 - $3.22\text{ }\mu\text{m}$) result from the presence of a bay region or a nitrogen atom within the PAH structure.

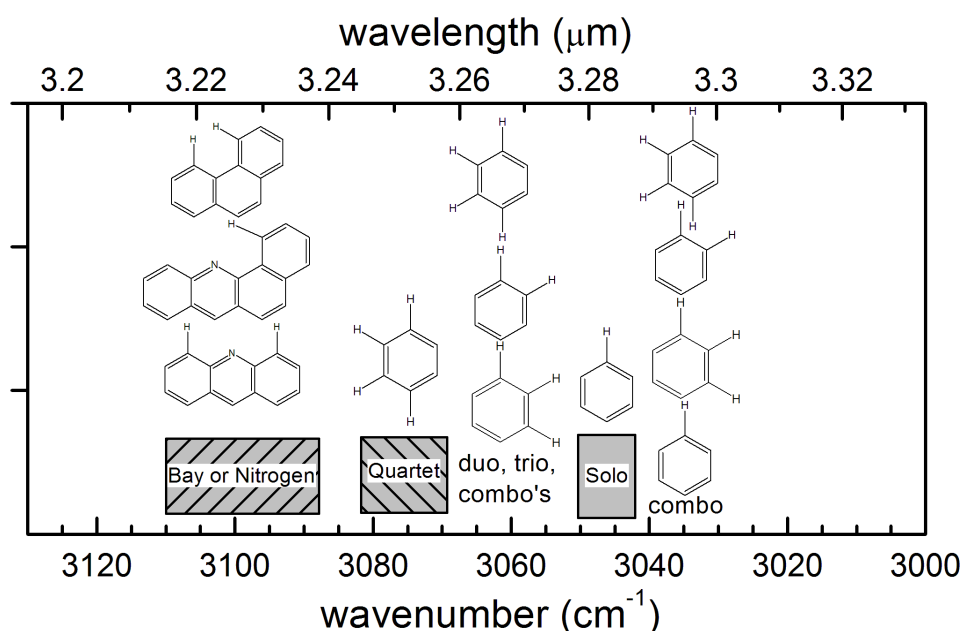


Figure 5: Summary of the C-H stretching region for the various PAH and PANH structures. Taken from Mattioda, et al. (2017).

Conclusions and Future Work

In conclusion, building on our earlier PANH IR work, the acridine series confirms the two-fold increase in band intensity observed for the 1100 - 1600 cm^{-1} (9.09 - $6.25\text{ }\mu\text{m}$) and further refines this increase to the 1375 - 1600 cm^{-1} (7.27 - $6.25\text{ }\mu\text{m}$) range. PANH molecules containing a C-H group para (opposite) the nitrogen atom exhibit an intense band around 1400 cm^{-1} ($7.14\text{ }\mu\text{m}$) and/or between ~ 1480 - 1515 cm^{-1} (6.76 - $6.60\text{ }\mu\text{m}$). The addition of the benzene rings to anthracene produces a splitting of the solo CHoop modes to a bay and external mode. The external solo C-H group tends to couple with the adjacent duo C-H groups, while the bay solo C-H tends to couple with the quartet groups. Thus, the incorporation and position of nitrogen atom impacts both the intensity and position of the CHoop modes. The incorporation of a nitrogen atom in the PAH as well as the addition of benzene rings impacts the number and

intensity of bands present in the 500-700 cm^{-1} region (i.e. skeletal modes). Quartet and solo C-H stretches fall around 3070 cm^{-1} (3.26 μm) and 3040 cm^{-1} (3.29 μm) respectively, with the trio and duo C-H stretches falling between this range. Incorporation of a nitrogen atom or the creation of a bay region in a PAH results in C-H stretching bands between 3090 and 3110 cm^{-1} (3.24-3.21 μm). **In summary, this study has shown that the presence of a nitrogen atom and its position in the PAH skeleton impacts PAH band positions and intensities, which could serve to help form an identification protocol to distinguish between PAHs and PANHs.**

Acknowledgements: This material is based upon work supported by the National Aeronautics and Space Administration through the NASA Astrobiology Institute under Cooperative Agreement Notice NNH13ZDA017C issued through the Science Mission Directorate.



Andy Mattioda is a research scientist at NASA Ames Research Center whose work focuses on understanding the prebiotic organic chemistry taking place in outer space and its potential relationship to the origins of life by investigating the infrared spectroscopy of organic molecules (especially Polycyclic Aromatic Hydrocarbons or PAHs) under interstellar conditions.

Email: andrew.mattioda@nasa.gov

References

- Gao, Juehan, et al. 2016, *The Journal of Physical Chemistry* 120, 7800
- Hudgins, D.M. & L.J. Allamandola 2004, *Astrophysics of Dust ASP Conf. Series*, 665
- Hudgins, D.M. & L.J. Allamandola 1999, *The Astrophysical Journal* 516, L41
- Hudgins, D.M. et al. 2005, *The Astrophysical Journal* 632, 316
- Kuan, Y. et al. 2003, *The Astrophysical Journal* 593, 848
- Mackie, C.J., et al. 2016, *The Journal of Physical Chemistry* 145, 084313-1
- Mattioda, A.L., Bauschlicher Jr., C.W., Ricca, A., Bregman, J., Hudgins, D.M., Allamandola, L.J. 2017, *Spectrochimica Acta Part A: Molecular and Biomolecular Spectroscopy* 181, 286-308
- Mattioda, A.L. et al. 2014, *Spectrochim. Acta A: Molecular Biomolecular Spec.* 130, 639
- Mattioda, A.L. et al. 2003, *The Journal of Physical Chemistry A* 107, 1486
- Mattioda, A.L. et al. 2005, *Advances in Space Research*, 156
- Peeters, Z. et al. 2003, *The Astrophysical Journal* 593, L129
- Pizzarello, S. 2001, *32nd Annual LPSC*. Houston, TX. Abstract No. 1886.
- Ricca, A. et al. 2001, *Icarus* 154, 516.
- Stoks, P.G. & Schwartz, A.W. 1982, *Geochimica Cosmochimica Acta* 46, 309

Abstracts

Extended Red Emission in IC 59 and IC 63

Thomas S. -Y. Lai¹, Adolf N. Witt¹ and Ken Crawford²

¹ Ritter Astrophysical Research Center, University of Toledo, Toledo, OH 43606, USA

² Rancho Del Sol Observatory, Camino, CA 95709, USA

We analysed new wide-field, wide- and narrow-band optical images of IC 59 and IC 63, two nebulae which are externally illuminated by the early B-star γ Cas, with the objective of mapping the extended red emission (ERE), a dust-related photoluminescence process that is still poorly understood, in these two clouds. The spatial distribution of the ERE relative to the direction of the incident radiation and relative to other emission processes, whose carriers and excitation requirements are known, provides important constraints on the excitation of the ERE. In both nebulae, we find the ERE intensity to peak spatially well before the more extended distribution of mid-infrared emission in the unidentified infrared bands, supporting earlier findings that point toward far-ultraviolet ($11 \text{ eV} < E_{\text{photon}} < 13.6 \text{ eV}$) photons as the source of ERE excitation. The band-integrated absolute intensities of the ERE in IC 59 and IC 63 measured relative to the number density of photons available for ERE excitation are lower by about two orders of magnitude compared to ERE intensities observed in the high-latitude diffuse interstellar medium (ISM). This suggests that the lifetime of the ERE carriers is significantly reduced in the more intense radiation field prevailing in IC 59 and IC 63, pointing toward potential carriers that are only marginally stable against photo-processing under interstellar conditions. A model involving isolated molecules or molecular ions, capable of inverse internal conversion and recurrent fluorescence, appears to provide the most likely explanation for our observational results.

E-mail: shaoyu.lai@utoledo.edu

Accepted for publication in MNRAS

<http://adsabs.harvard.edu/abs/2017arXiv170504313L>

Photoionization Efficiencies of Five Polycyclic Aromatic Hydrocarbons

K. Olof Johansson¹, Matthew F. Campbell¹, Paolo Elvati², Paul E. Schrader¹, Judit Zádor¹, Nicole K. Richards-Henderson³, Kevin R. Wilson³, Angela Violi^{2,4}, and Hope A. Michelsen¹

¹Combustion Research Facility, Sandia National Laboratories, Livermore, California 94550, United States

²Department of Mechanical Engineering, University of Michigan, Ann Arbor, Michigan 48109, United States

³Chemical Sciences Division, Lawrence Berkeley National Laboratory, Berkeley, California 94720, United States

⁴Departments of Chemical Engineering, Macromolecular Science and Engineering, Biophysics Program, University of Michigan, Ann Arbor, Michigan 48109, United States

We have measured photoionization-efficiency curves for pyrene, fluoranthene, chrysene, perylene, and coronene in the photon energy range of 7.5-10.2 eV and derived their photoionization cross-section curves in this energy range. All measurements were performed using tunable vacuum ultraviolet (VUV) radiation generated at the Advanced Light Source synchrotron at Lawrence Berkeley National Laboratory. The VUV radiation was used for photoionization, and detection was performed using a time-of-flight mass spectrometer. We measured the photoionization efficiency of 2,5-dimethylfuran simultaneously with those of pyrene, fluoranthene, chrysene, perylene, and coronene to obtain references of the photon flux during each measurement from the known photoionization cross-section curve of 2,5-dimethylfuran.

E-mail: Hope A. Michelsen (hamiche@sandia.gov), K. Olof Johansson (okjohan@sandia.gov)

J. Phys. Chem. A, 2017, 121 (23)

<http://pubs.acs.org/doi/abs/10.1021%2Facs.jpca.7b02991>

Kekulene: Structure, Stability and Nature of H•••H Interactions in Large PAHs

J. Poater^{a,b}, J. Paauwe^c, S. Pan^d, G. Merino^d, C. Fonseca Guerra^{c,e}, F.M. Bickelhaupt^{c,f}

^a Departament de Química Inorgànica i Orgànica & IQTCUB, Universitat de Barcelona, Martí i Franquès 1-11, 08028 Barcelona, Catalonia, Spain

^b ICREA, Pg. Lluís Companys, 23, 08010 Barcelona, Spain

^c Department of Theoretical Chemistry and Amsterdam Center for Multiscale Modeling (ACMM), Vrije Universiteit Amsterdam, De Boelelaan 1083, NL-1081 HV Amsterdam, The Netherlands

^d Departamento de Física Aplicada, Centro de Investigación y de Estudios Avanzados Unidad Mérida, Km. 6 Antigua carretera a Progreso, Apdo. Postal 73, Cordemex, 97310, Mérida, Yuc., México

^e Leiden Institute of Chemistry, Gorlaeus Laboratories, Leiden University, P.O. Box 9502, 2300 RA Leiden, Netherlands

^f Institute of Molecules and Materials (IMM), Radboud University, Heyendaalseweg 135, NL-6525 AJ Nijmegen, The Netherlands

We have quantum chemically analyzed how the stability of small and larger polycyclic aro-

matic hydrocarbons (PAHs) is determined by characteristic patterns in their structure using density functional theory at the BLYP/TZ2P level. In particular, we focus on the effect of the nonbonded H•••H interactions that occur in the bay region of kinked (or armchair) PAHs, but not in straight (or zigzag) PAHs. Model systems comprise anthracene, phenanthrene, and kekulene as well as derivatives thereof. Our main goals are: (1) to explore how nonbonded H•••H interactions in armchair configurations of kinked PAHs affect the geometry and stability of PAHs and how their effect changes as the number of such interactions in a PAH increases; (2) to understand the extent of stabilization upon the substitution of a bay C–H fragment by either C• or N; and (3) to examine the origin of such stabilizing/destabilizing interactions.

E-mail: jordi.poater@ub.edu

Molecular Astrophysics 2017, 8, 19

<http://www.sciencedirect.com/science/article/pii/S2405675816300513>

B-DNA Model Systems in Non-Terran Bio-Solvents: Implications for Structure, Stability and Replication

Trevor A. Hamlin^a, Jordi Poater^{b,c}, Célia Fonseca Guerra^{a,d},
F. Matthias Bickelhaupt^{a,e}

^a Department of Theoretical Chemistry and Amsterdam Center for Multiscale Modeling (ACMM), Vrije Universiteit Amsterdam, De Boelelaan 1083, NL-1081 HV Amsterdam, The Netherlands

^b Departament de Química Inorgànica i Orgànica & Institut de Química Teòrica i Computacional (IQTCUB), Universitat de Barcelona, Martí i Franquès 1-11, 08028 Barcelona, Catalonia, Spain

^c ICREA, Pg. Lluís Companys, 23, 08010 Barcelona, Spain

^d Leiden Institute of Chemistry, Gorlaeus Laboratories, Leiden University, P.O. Box 9502, 2300 RA Leiden, Netherlands

^e Institute of Molecules and Materials (IMM), Radboud University, Heyendaalseweg 135, NL-6525 AJ Nijmegen, The Netherlands

We have computationally analyzed a comprehensive series of Watson-Crick and mismatched B-DNA base pairs, in the gas phase and in several solvents, including toluene, chloroform, ammonia, methanol and water, using dispersion-corrected density functional theory and implicit solvation. Our analyses shed light on how the molecular-recognition machinery behind life's genetic code depends on the medium, in order to contribute to our understanding of the possibility or impossibility for life to exist on exoplanetary bodies. Calculations show how a common non-terran environment like ammonia, less polar than water, exhibits stronger hydrogen-bonding affinities, although showing reduced selectivities towards the correct incorporation of Watson-Crick base pairs into the backbone. Thus, we prove the viability of DNA replication in a non-terran environment.

E-mail: t.a.hamlin@vu.nl

Phys. Chem. Chem. Phys., 2017, Advance Article

<http://pubs.rsc.org/en/content/articlepdf/2017/cp/c7cp01908d>

Dehydrogenation effects on the stability of aromatic units in polycyclic aromatic hydrocarbons in the interstellar medium: A computational study at finite temperature

P. Parneix^a, A. Gambo^{a,b}, C. Falvo^a, M.A. Bonnin^a, T. Pino^a, F. Calvoc^c

^a Institut des Sciences Moléculaires d'Orsay, CNRS, Univ. Paris-Sud, Université Paris-Saclay, F-91405 Orsay, France

^b Centro de Investigaciones Químicas (CIQ), Universidad Autónoma del Estado de Morelos (UAEM), Cuernavaca, Morelos, 62209 México

^c Univ. Grenoble Alpes, LIPHY, F-38000 Grenoble, France and CNRS, Liphy, F-38000 Grenoble, France

Isomerization, ionization and fragmentation of molecular compounds in the interstellar medium can be triggered by stellar radiation and cosmic rays. In the present contribution, we examine the propensity for isomerization and the relative stability of aromatic rings in the pyrene and coronene molecules at various degrees of dehydrogenation by means of molecular modeling. Using the AIREBO reactive force field and advanced Monte Carlo techniques such as the Wang-Landau method based on suitable order parameters, entire free-energy profiles describing the isomerization pathways and equilibrium properties were calculated as a function of temperature or total energy. We generally find that hydrogenation significantly stabilizes the fully polycyclic aromatic hydrocarbon (PAH) structure, even though local dehydrogenation next to an aromatic ring favors ring opening. The formation of pentagonal rings, a typical defect motif in the polycyclic carbon skeleton, is predicted to be actually competitive with the loss of a hydrogen atom. Our investigation emphasizes the likely presence of defects in astrophysical PAHs, whose spectral features remain to be better characterized and understood.

E-mail: pascal.parneix@u-psud.fr

Molecular Astrophysics, 2017, 7, 9

<http://www.sciencedirect.com/science/article/pii/S2405675816300495>

Laboratory spectroscopy and astronomical significance of the fully-benzenoid PAH triphenylene and its cation

V. Kofman^{a,b}, P.J. Sarre^c, R.E. Hibbins^{c,d}, I.L. ten Kate^b, H. Linnartz^a

^aSackler Laboratory for Astrophysics, Leiden Observatory, Leiden University, PO Box 9513, 2300 RA Leiden, The Netherlands

^bDepartment of Earth Sciences, Utrecht University, Budapestlaan 4, 3584 CD Utrecht, The Netherlands

^cSchool of Chemistry, The University of Nottingham, University Park, Nottingham NG7 2RD, United Kingdom

^dDepartment of Physics, Norwegian University of Science and Technology, N-7491 Trondheim, Norway

Triphenylene (C₁₈H₁₂) is a highly symmetric polycyclic aromatic hydrocarbon (PAH) molecule with a “fully-benzenoid” electronic structure. This confers a high chemical stability compared with PAHs of similar size. Although numerous infrared and UV-vis experimental spectroscopic and theoretical studies of a wide range PAHs in an astrophysical context have been conducted, triphenylene and its radical cation have received almost no attention. There exists a huge

body of spectroscopic evidence for neutral and ionised PAHs in astrophysical sources, obtained principally through detection of infrared emission features that are characteristic of PAHs as a chemical class. However, it has so far not proved possible to identify spectroscopically a single isolated PAH in space, although PAHs including triphenylene have been detected mass spectrometrically in meteorites. In this work we focus on recording laboratory electronic spectra of neutral and ionised triphenylene between 220 and 780 nm, trapped in H₂O ice and solid argon at 12 K. The studies are motivated by the potential for spectroscopic astronomical detection of electronic absorption spectra of PAHs in ice mantles on interstellar grains as discussed by Linnartz (2014), and were performed also in a cold Ar matrix to provide guidance as to whether triphenylene (particularly in its singly positively ionised form) could be a viable candidate for any of the unidentified diffuse interstellar absorption bands. Based on the argon-matrix experimental results, comparison is made with previously unpublished astronomical spectra near 400 nm which contain broad interstellar absorption features consistent with the predictions from the laboratory matrix spectra, thus providing motivation for the recording of gas-phase electronic spectra of the internally cold triphenylene cation.

E-mail: kofman@strw.leidenuniv.nl

Molecular Astrophysics 2017, 7, 19

<http://www.sciencedirect.com/science/article/pii/S2405675817300039>

Symmetry Breaking and Spectral Considerations of the Surprisingly Floppy *c*-C₃H Radical and the Related Dipole-Bound Excited State of *c*-C₃H⁻

Matthew K. Bassett¹ and Ryan C. Fortenberry¹

¹ Georgia Southern University, Department of Chemistry and Biochemistry, Statesboro, GA 30460 U.S.A.

The C₃H radical is believed to be prevalent throughout the interstellar medium (ISM) and may be involved in the formation of polycyclic aromatic hydrocarbons. C₃H exists as both a linear and a cyclic isomer. The C_{2v} cyclopropanylidenyl radical isomer was detected in the dark molecular cloud TMC-1, and the linear propanylidenyl radical isomer has been observed in various dark molecular clouds. Even though *c*-C₃H radical has been classified rotationally, the vibrational frequencies of this seemingly important interstellar molecule have never been directly observed. Established, highly-accurate quartic force field methodologies are employed here to compute useful geometrical data, spectroscopic constants, and vibrational frequencies. The computed rotational constants are consistent with the experimental results. Consequently, the three *a*₁ (ν_1 , ν_2 , and ν_3) and one *b*₁ (ν_6) anharmonic vibrational frequencies at 3117.7 cm⁻¹, 1564.3 cm⁻¹, 1198.5 cm⁻¹, and 826.7 cm⁻¹, respectively, are reliable predictions for these, as of yet unseen, observables. Unfortunately, the two *b*₂ fundamentals (ν_4 and ν_5) cannot be treated adequately in the current approach due to a flat and possible double-well potential described in detail herein. The dipole-bound excited state of the anion suffers from the same issues and may not even be bound. However, the trusted fundamental vibrational frequencies described for the neutral radical should not be affected by this deformity and are the first robustly produced

for $c\text{-C}_3\text{H}$. The insights gained here will also be applicable to other structures containing three-membered bare and exposed carbon rings that are surprisingly floppy in nature.

E-mail: rfortenberry@georgiasouthern.edu

Journal of Chemical Physics, 146, 224303 (2017)

<http://aip.scitation.org/doi/full/10.1063/1.4985095>

Structure and Dissociation Pathways of Protonated Tetralin (1,2,3,4-Tetrahydronaphthalene)

Martin Vala¹, Jos Oomens² and Giel Berden²

¹ Department of Chemistry and Center for Chemical Physics, University of Florida, Gainesville, Florida 32611-7200, United States

² Radboud University, Institute for Molecules and Materials, FELIX Laboratory, Toernooiveld 7c, NL-6525 ED Nijmegen, The Netherlands

The infrared multiple-photon dissociation (IRMPD) spectrum of protonated tetralin (1,2,3,4-tetrahydronaphthalene, THN) has been recorded using an infrared free electron laser coupled to a Fourier transform ion cyclotron mass spectrometer. IR-induced fragmentation of the protonated parent $[\text{THN} + \text{H}]^+$, m/z 133, yielded a single fragment ion at m/z 91. No evidence for fragment ions at m/z 131 or 132 was observed, indicating that protonated THN ejects neither atomic H nor molecular H_2 . Comparison of the experimental spectrum with density functional calculations (B3LYP/6-311++G(d,p)) of the two possible protonated isomers identifies a preference for the position of protonation. Possible decomposition pathways starting from both $[\text{THN} + \text{H}(5)]^+$ and $[\text{THN} + \text{H}(6)]^+$ are investigated. The potential energy profiles computed for these decomposition routes reveal that (1) the m/z 91 ionic product resembles the benzylium ion, but with the extra hydrogen and the methylene substituents in various *ortho*, *meta*, and *para* conformations around the aromatic ring and that (2) the decomposition process involving the $[\text{THN} + \text{H}(6)]^+$ isomer is predominant, while the one involving the $[\text{THN} + \text{H}(5)]^+$ may play a smaller role. Potential energy pathways from the initial decomposition product(s) to the benzylium and tropylium ions have also been computed. Given the relatively low barriers to these ions, it is concluded that the benzylium ion and, with sufficient activation, the tropylium ion plus neutral propene are the final products.

E-mail: mvala@chem.ufl.edu

Accepted for publication in J. Phys. Chem. A

<http://dx.doi.org/10.1021/acs.jpca.7b01858>

AstroPAH Newsletter

<http://astropah-news.strw.leidenuniv.nl>
astropah@strw.leidenuniv.nl

Next issue: 18 July 2017
Submission deadline: 7 July 2017